ACS central science

http://pubs.acs.org/journal/acscii

Research Article

# Stabilization of the Dinitrogen Analogue, Phosphorus Nitride

Jorge L. Martinez, Sean A. Lutz, Daniel M. Beagan, Xinfeng Gao, Maren Pink, Chun-Hsing Chen, Veronica Carta, Pierre Moënne-Loccoz, and Jeremy M. Smith*

Cite This: *ACS Cent. Sci.* 2020, 6, 1572–1577

Read Online

ACCESS | Metrics & More | Article Recommendations | Supporting Information

**ABSTRACT:** The $N_2$ analogue phosphorus nitride (PN) was the first phosphorus-containing compound to be detected in the interstellar medium; however, this thermodynamically unstable compound has a fleeting existence on Earth. Here, we show that reductive coupling of iron(IV) nitride and molybdenum(VI) phosphide complexes assembles PN as a bridging ligand in a structurally characterized bimetallic complex. Reaction with C≡N$^t$Bu releases the mononuclear complex $[(N_3N)Mo—PN]^-$, $N_3N$ = $[(Me_3SiNCH_2CH_2)_3N]^{3-}$), which undergoes light-induced linkage isomerization to provide $[(N_3N)Mo—NP]^-$, as revealed by photocrystallography. While structural and spectroscopic characterization, supported by electronic structure calculations, reveals the PN multiple bond character, coordination to molybdenum induces a nucleophilic character at the terminal atom of the PN/NP ligands. Indeed, the linkage isomers can be trapped in solution by reaction with a Rh(I) electrophile.

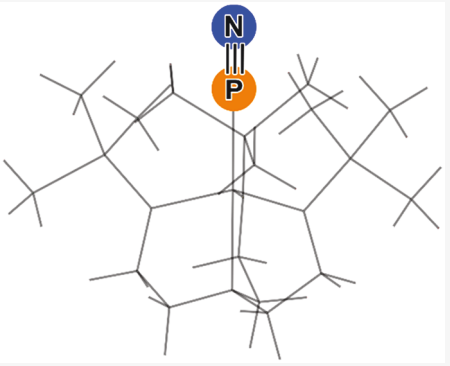


The $N_2$ analogue phosphorus nitride (PN) was the first phosphorus-containing compound to be detected in the interstellar medium.[1] On Earth, PN was first spectroscopically observed in the gas phase[2,3] and later isolated in frozen Kr matrices.[4] Even under these cryogenic conditions, the compound is not stable above 10 K, irreversibly aggregating to $D_{3h}$ $P_3N_3$[5] in a noble gas matrix, and polymerizing to $[PN]_n$ in its absence. The thermodynamic instability of PN is further underscored by the results of *ab initio* calculations that show that its formation from $N_2$ and $P_2$ is endergonic.[6]

Complexation to transition metals is a common strategy for stabilizing unstable molecules. For example, while $P_2$ has a fleeting existence in room temperature solution,[7] numerous $P_2$ complexes have been synthesized and characterized, including by single crystal X-ray diffraction.[8] Despite the fact that vibrational spectroscopy provides evidence that PN can interact with metal atoms in Kr matrices,[9] isolable PN complexes are still unknown. The only evidence for a PN complex is provided by a trinuclear cyclotriphosphane complex that serves as a synthon for the unobserved species $(Ar^tBuN)_3V—N≡P$ (Ar = 3,5-$Me_2C_6H_3$) in solution.[10] Isolable complexes will provide insight into the molecular and electronic structure of coordinated PN as well as establish a platform for its use in chemical synthesis.

We have reported on isolable, yet reactive, iron(IV) nitride complexes supported by tripodal *N*-heterocyclic carbene (NHC) ligands.[11] These complexes are reactive in reductive coupling reactions that allow for the assembly of multinuclear complexes and diatomic ligands.[12,13] Here, we report that this reductive coupling strategy can be extended to the assembly of PN, allowing for the physical and chemical properties of this ligand to be investigated for the first time.

Reaction of the four-coordinate iron(IV) nitride complex, $PhB(^iPr_2Im)_3Fe≡N$ ($PhB(^iPr_2Im)_3$ = phenyltris(3,4-diisopropylimidazol-2-ylidene)borato),[13] with the previously reported molybdenum(VI) phosphide, $(N_3N)Mo≡P$ ($N_3N$ = $[(Me_3SiNCH_2CH_2)_3N]^{3-}$),[14,15] provides the olive green complex $PhB(^iPr_2Im)_3Fe—N=P—Mo(N_3N)$ (**1**) in high yield (Figure 1). The molecular structure of **1**, as determined by single crystal X-ray diffraction, reveals a very short P—N distance of 1.509(6) Å (Figure 1). This distance is slightly longer than that determined by microwave spectroscopy for gas phase phosphorus nitride (1.490 86(2) Å),[16,17] and over 0.1 Å shorter than in nonmetallic carbene-stabilized PN compounds,[18] which is consistent with the PN multiple bond character. The short Mo—P distance (2.179(2) Å) and linear Mo—P—N angle (179.2(3) °) also suggest the multiple bond character between these two atoms.

The isomer shift ($\delta$ = 0.63(2) mm/s) and quadrupole splitting ($\Delta E_Q$ = 1.62(2) mm/s) in the solid-state $^{57}$Fe Mössbauer spectrum of **1** are both similar to the parameters observed for other high-spin Fe(II) tris(carbene)borate complexes (Figure S17).[19] Consistent with this formulation, **1** is paramagnetic, with a solution magnetic moment ($\mu_{eff}$ = 4.9(3) $\mu_B$) arising from the high-spin ($S$ = 2) iron(II) center.

**Received:** July 17, 2020
**Published:** September 1, 2020

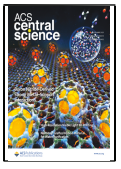









https://dx.doi.org/10.1021/acscentsci.0c00944
*ACS Cent. Sci.* 2020, 6, 1572–1577

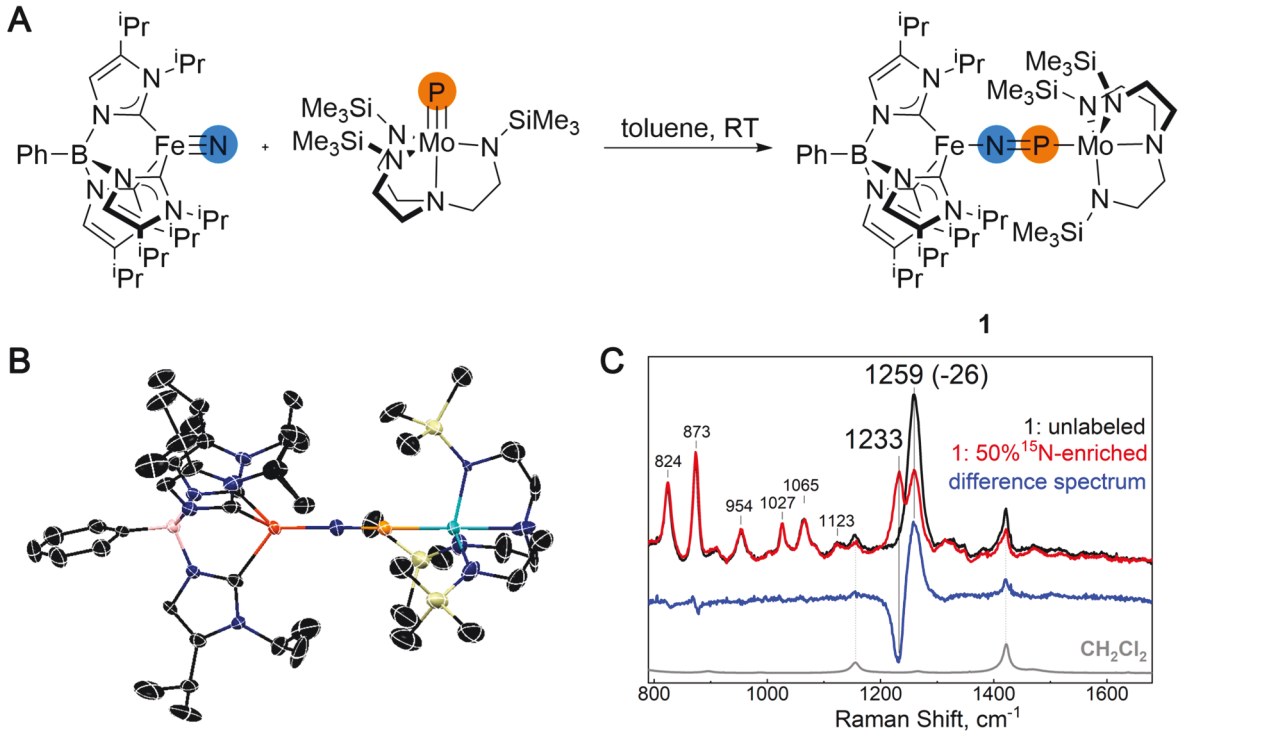


**Figure 1.** (A) Synthesis of complex **1** by reductive coupling of Fe(IV) nitrido and Mo(VI) phosphido complexes. (B) X-ray crystal structure of **1**, thermal ellipsoids at 50% probability. Black, blue, pink, teal, orange, and yellow ellipsoids represent carbon, nitrogen, boron, molybdenum, phosphorus, and silicon atoms, respectively. (C) Resonance Raman spectra of **1** in $CH_2Cl_2$ at room temperature for samples prepared with unlabeled (black trace) and 50% $^{15}$N-enriched PhB($^i$Pr$_2$Im)$_3$Fe≡N (red trace).

Resonance Raman spectroscopy supports the PN multiple bond character. Resonance Raman spectra of **1** in $CH_2Cl_2$ obtained with a 407 nm laser excitation identify an intense band at 1259 cm$^{-1}$ that shifts to 1233 cm$^{-1}$ with a $^{15}$N-enriched sample (Figure 1). The 1259 cm$^{-1}$ frequency compares well with the stretching frequency of free PN ($\nu_{PN}$ = 1323 cm$^{-1}$),[4] and its −26 cm$^{-1}$ isotope downshift with $^{15}$N matches the expectation from Hooke's law for a P−N harmonic oscillator (calculated $\Delta^{15}$N = −29 cm$^{-1}$).

The lability of the high-spin iron(II) center in **1** allows the PN ligand to be deprotected. Addition of 3 equiv. of C≡N$^t$Bu quantitatively yields the orange-yellow salt [PhB($^i$Pr$_2$Im)$_3$Fe(C≡N$^t$Bu)$_3$][(N$_3$N)Mo(PN)] (**2**). The identity of **2** is confirmed by single crystal X-ray diffraction, with the solid-state structure revealing positional disorder of the PN ligand. For the major component (**2a**, 70% occupancy), molybdenum retains the connectivity of complex **1**, with the PN ligand bound to the metal through the phosphorus atom (Figure 2). While the P—N and Mo—P bond lengths are both slightly longer than in **1**, the Mo—P—N linkage remains linear, and the structural metrics suggest that the P—N and Mo—P multiple bond character is maintained.

The minor component (**2b**, 30% occupancy) is the linkage isomer of **2a**, where molybdenum is bound to the nitrogen atom of the PN ligand (Figure 2). A photocrystallographic experiment reveals that the formation of **2b** is photochemically induced in the solid state. Here, a series of experiments in which a single crystal of **2** is exposed to white light, followed by data collection in the dark, reveal the loss of **2a** with concomitant formation of **2b** (Figures S27−S29 and Table S3). After 25 h of exposure to white light, isomer **2a** is the minor component (24% occupancy) and **2b** the major component (76% occupancy). For **2b**, the P−N bond length

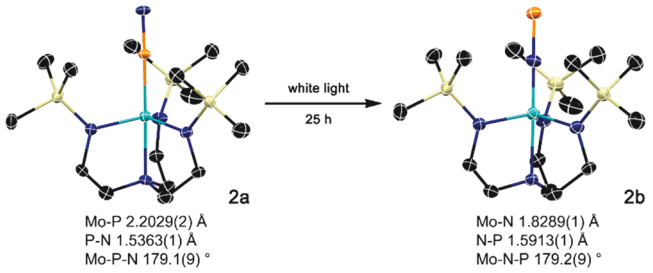


**Figure 2.** Photocrystallographic characterization of the conversion of **2a** to **2b** by PN linkage isomerization. Thermal ellipsoids shown at 50% probably, hydrogen atoms omitted for clarity. Carbon, molybdenum, nitrogen, phosphorus, and silicon atoms shown as black, teal, blue, orange, and yellow ellipsoids, respectively.

is greater than in **2a**, while the Mo−N bond length is similar to those observed in related molybdenum diazenido complexes.[20,21] The Mo−N−P linkage is also linear. Together, these structural data suggest that the phosphorus−nitrogen multiple bond character is maintained in **2b**, but that the NP linkage isomer is a better $\pi$-acid. The outcome of the photoisomerization reaction is consistent with DFT calculations that reveal that the linkage isomer **2b** is thermodynamically favored but with a large barrier toward thermally driven intramolecular isomerization (Figure S25).

The solid-state structures of **2a** and **2b** reveal that PN is not sterically protected by the tris(amido)amine ligand, suggesting that the ligand is electronically stabilized. The electronic structure of **2a**, as determined by DFT (def2-tzvp/B3LYP/dkh2) reveals that the two highest occupied molecular orbitals of **2a** are perpendicular combinations of the molybdenum 4d$_{xz}$/4d$_{yz}$ and PN $\pi/\pi^*$ orbitals (Figure 3A,B, Figure S23).


https://dx.doi.org/10.1021/acscentsci.0c00944
ACS Cent. Sci. 2020, 6, 1572−1577

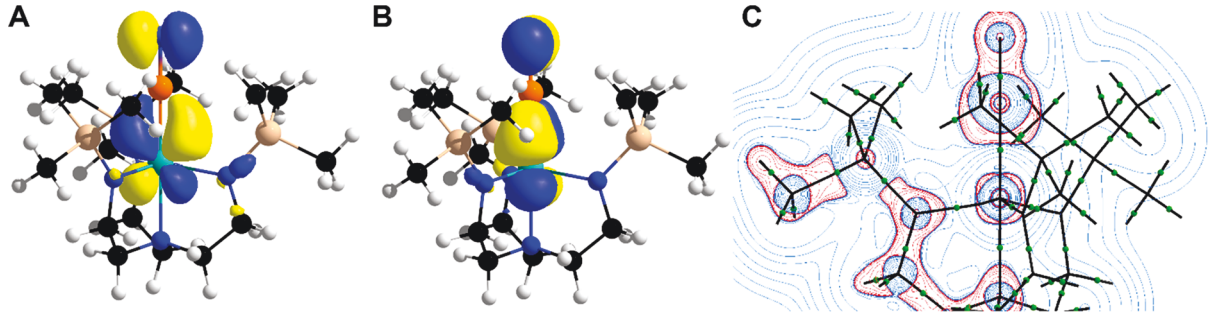


**Figure 3.** (A) HOMO, and (B) HOMO-1 of **2a**, as calculated by density functional theory (def2-tzvp/B3LYP/dkh2) with isodensity 0.05. (C) Contour plot of the Laplacian of the electron-density topology ($\nabla^2(\rho)$) of **2a**. Blue curves show areas of charge depletion; red curves show areas of charge concentration. Green spheres show bond critical points.

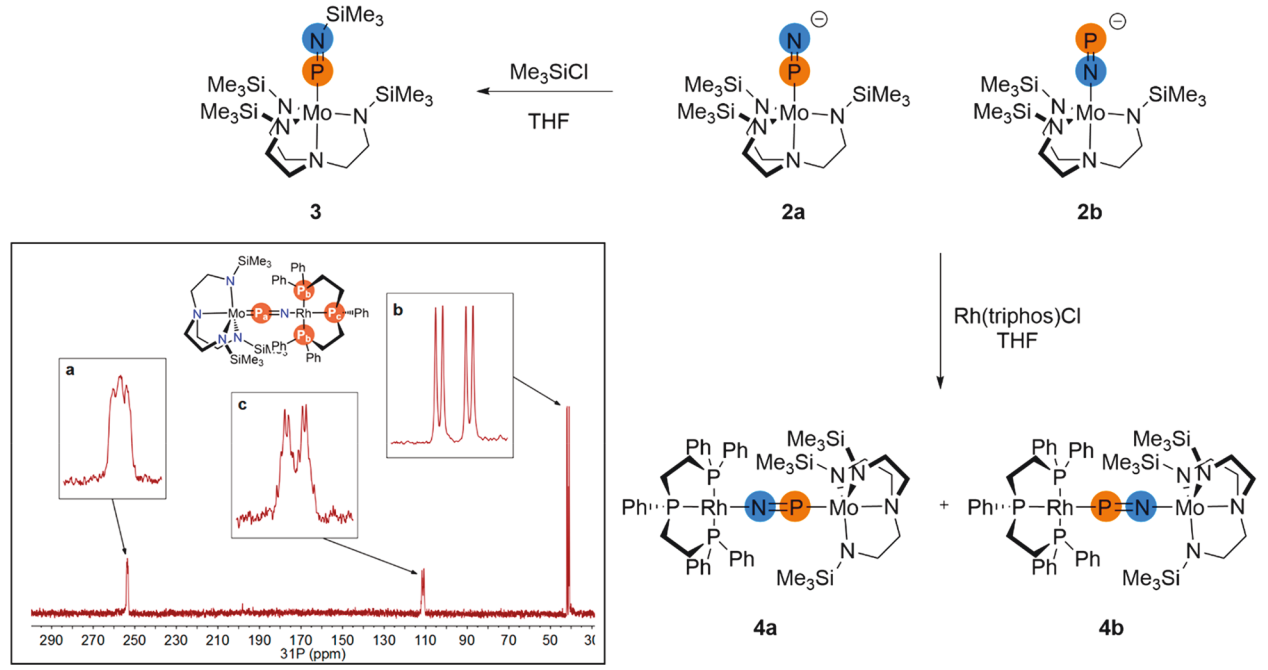


**Figure 4.** Reactivity of **2**. Inset: $^{31}P\{^1H\}$ NMR spectrum of **4a**, showing assignments of the resonances.

This $\pi$-backbonding interaction stabilizes the PN ligand without significantly reducing its triple bond character. This is supported by the results of a natural bond orbital (NBO) analysis, which indicates the presence of a PN triple bond that is polarized toward the nitrogen atom, with a Wiberg bond index of 2.145 (Table S1).[22] A topological analysis[23] reveals a very small ellipticity ($\varepsilon$ = 0.000 032) for the PN ligand, consistent with a cylindrically symmetric bond. The Laplacian ($\nabla^2(\rho)$ = 1.347) shows charge depletion between phosphorus and nitrogen, indicating a polar bond (Figure 3, Table S2). DFT calculations suggest a similar electronic structure for the linkage isomer **2b**; however, NBO analysis indicates a single bond that is polarized toward the N atom, with a Wiberg bond index of 0.392 (Table S1). This is similar to the proposed formulation of the NP ligand in the transient species $(Ar^tBuN)_3V{-}N{\equiv}P$ (Ar = 3,5-$Me_2C_6H_3$).[10] Consistent with this, topological analysis reveals that the NP ligand in **2b** is also cylindrically symmetric ($\varepsilon$ = 0.000 022), although less polarized than the PN ligand, with $\nabla^2(\rho)$ = 0.552 (Table S3). Importantly, the electronic structures of **2a** and **2b** predict the terminal atom of the PN/NP ligand in both complexes to be the locus of nucleophilic reactivity. The computations also reveal that end-on binding of the PN/NP ligand is significantly more favorable than the side-on isomer. The coordination preference of PN/NP in **2** is therefore akin to that of $N_2$ rather than $P_2$.

Additional calculations reveal that **2a** and **2b** have a similar electronic structure to those of their isoelectronic congeners $[(N_3N)Mo(L)]^-$ (L = $N_2$, $P_2$, CO) and $[(N_3N)Mo(PO)]$ (Figure S24). However, a topological analysis[23] reveals that ligand polarization increases from PP to PN to PO based on the magnitude of the ($\nabla^2(\rho)$),[23] following the electronegativities of the terminal atoms (Figure S25 and Table S2). The large positive value of ($\nabla^2(\rho)$) for PN suggests a polarized bond that is closer in nature to the highly polarized PO ligand. These ligands have similar electron densities at the bond critical points ($\rho$) and bond ellipticities ($\varepsilon$) of essentially zero, suggesting that all ligands have cylindrical electron densities. Similarly, an increase in polarization of the ligand is observed from NN to NP and CO based on the magnitude of ($\nabla^2(\rho)$), with the two latter ligands having similar polarity (Table S3). The values of $\rho$ and $\varepsilon$ are also consistent with having cylindrical electron densities.


https://dx.doi.org/10.1021/acscentsci.0c00944
ACS Cent. Sci. 2020, 6, 1572−1577

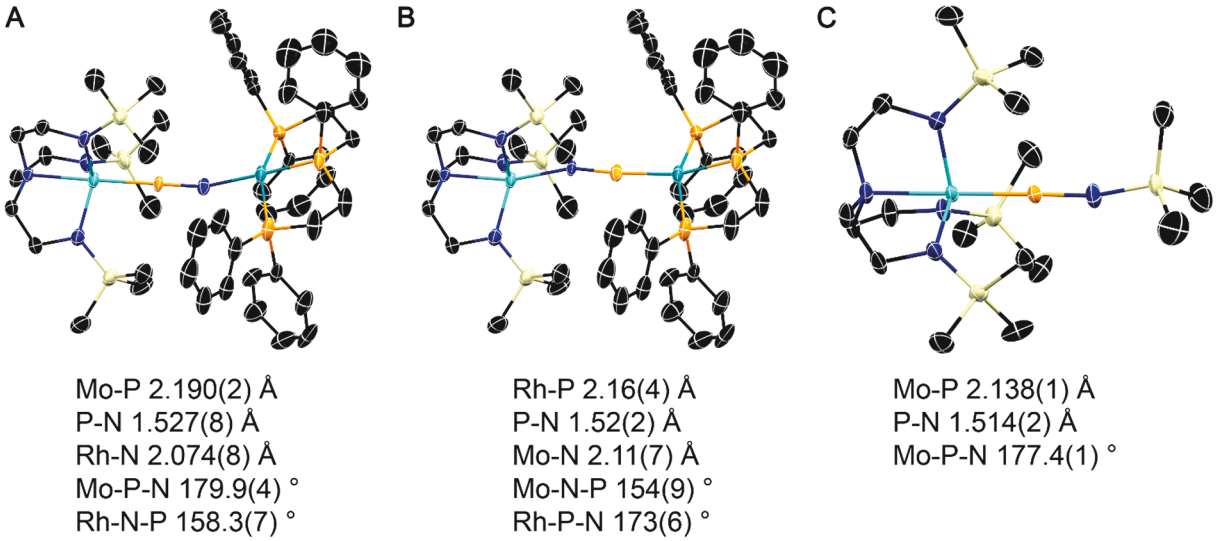


**Figure 5.** X-ray crystal structures of (A) **3a**, (B) **3b**, and (C) **4**. Thermal ellipsoids shown at 50% probability, hydrogen atoms omitted for clarity. Carbon, molybdenum, nitrogen, phosphorus, rhodium, and silicon atoms shown as black, teal, blue, orange, aquamarine, and yellow ellipsoids, respectively.

The diamagnetic nature of **2** allows the PN ligand to be characterized by multinuclear NMR spectroscopy. A single resonance is observed at $\delta$ 312 ppm in the $^{31}P\{^{1}H\}$ NMR spectrum of **2**, significantly upfield from that observed for the molybdenum(VI) phosphide starting complex $(N_3N)Mo{\equiv}P$,[15] but similar to that observed for the phosphorus monoxide complex $(^{t}BuNAr)_3Mo{=}P{=}O$,[24] in which the phosphorus atom is also two-coordinate. A doublet at $\delta$ 445 pm ($^{1}J_{NP}$ = 105 Hz) is observed in the $^{15}N$ NMR spectrum for isotopically enriched complex (**2-$^{15}$N**, 50%), revealing that the PN bond remains intact in solution (Figure S5). Variable temperature NMR experiments do not definitively exclude the possibility of rapid linkage isomerization on the time scale of the experiment, although as noted above, computational investigations suggest that an intramolecular isomerization mechanism involving a side-on PN ligand is thermally inaccessible. Attempts to characterize **2** by resonance Raman spectroscopy were unsuccessful as laser irradiation converts **2** to a molybdenum nitride species (Figure S22).

While spectroscopic data do not provide evidence for PN linkage isomerization in solution, the two isomers can be trapped by reaction with a soft electrophile (Figure 4). Specifically, reaction of **2** with (triphos)RhCl[25] (triphos = $PhP\{CH_2CH_2PPh_2\}_2$) provides a mixture of the bimetallic complexes $(N_3N)Mo{-}PN{-}Rh$(tripos) **3a** and $(N_3N)Mo{-}NP{-}Rh$(tripos) **3b**, along with the salt $[PhB(^{i}Pr_2Im)_3Fe(C{\equiv}N^{t}Bu)_3]Cl$. The molecular structures of the bimetallic complexes were determined by single crystal XRD, with the isomers **3a** (Figure 5A) and **3b** (Figure 5B) cocrystallizing in a 94:6 ratio. While positional disorder of the PN results in larger standard uncertainties for the geometrical parameters, it is evident that coordination to Rh slightly decreases the PN distance for both isomers. The PN ligand is linear at phosphorus and bent at nitrogen for both complexes.

Spectroscopic characterization confirms the existence of these two isomers in solution. Most notably, three sets of resonances are observed in the $^{31}P\{^{1}H\}$ NMR spectra of both **3a** (Figure 4, inset) and **3b**, in accord with the solid-state structures. The connectivity of the phosphorus nitride ligand in **3a** has been established through a series of homodecoupling and variable temperature $^{31}P\{^{1}H\}$ NMR experiments (Figures S10−S19), allowing the resonance at $\delta$ 253.5 ppm ($^{1}J_{RhP}$ = 135 Hz, $^{2}J_{PP}$ = 36 Hz, $^{3}J_{PN}$ = 29 Hz) to be assigned to the phosphorus atom of the PN ligand. Similarly, the phosphorus nitride resonance for **3b** is assigned as $\delta$ 258.1 ppm in the $^{13}P\{^{1}H\}$ NMR spectrum. There is no evidence for the interconversion **3a** and **3b** (indeed **3b** slowly decomposes in solution), which when combined with the solution spectral data implicates the presence of both **2a** and **2b** in solution.

The formation of **3a** and **3b** is consistent with the anticipated nucleophilic character of the terminal atom of the PN ligand **2a** and **2b**. This nucleophilic character also allows for the functionalization of PN by nonmetallic substrates. In an initial demonstration, reaction of **2** with excess $Me_3SiCl$ provides the yellow diamagnetic complex **4** as the sole molybdenum-containing product (Figure 4). The solid-state structure of **4** reveals that silylation results in a slight elongation of the P−N bond and contraction of the Mo−P bond (Figure 5C). The $^{31}P\{^{1}H\}$ NMR resonance of **4** is shifted upfield from **2** to $\delta$ 199 ppm, with the resonance in the $^{15}N$ NMR spectrum shifted upfield to $\delta$ 193 ppm ($^{1}J_{NP}$ = 72 Hz). The smaller one-bond coupling constant for **4**, as compared with that in **2**, is consistent with the observed P−N bond elongation. Functionalization of the PN ligand occurs at the terminal atom, in accord with the predictions from the electronic structure.

Reductive coupling of terminal phosphide and nitride ligands provides access to a sterically accessible and reactive PN ligand that is stabilized by $\pi$-backbonding. While the multiple bond character of free PN is retained in one linkage isomer, the stabilized diatomic is reactive toward further functionalization at either phosphorus or nitrogen. The synthetic strategy used to prepare PN is expected to stabilize other diatomic molecules that have an otherwise fleeting existence.

## ■ ASSOCIATED CONTENT

### Supporting Information

The Supporting Information is available free of charge at https://pubs.acs.org/doi/10.1021/acscentsci.0c00944.



https://dx.doi.org/10.1021/acscentsci.0c00944
ACS Cent. Sci. 2020, 6, 1572−1577

Full synthetic, spectroscopic, crystallographic, and computational details (PDF)

Crystal structures (CIF)

## AUTHOR INFORMATION


### Corresponding Author

**Jeremy M. Smith** − *Department of Chemistry, Indiana University, Bloomington, Indiana 47405, United States;* orcid.org/0000-0002-3206-4725; Email: smith962@indiana.edu

### Authors

**Jorge L. Martinez** − *Department of Chemistry, Indiana University, Bloomington, Indiana 47405, United States*

**Sean A. Lutz** − *Department of Chemistry, Indiana University, Bloomington, Indiana 47405, United States*

**Daniel M. Beagan** − *Department of Chemistry, Indiana University, Bloomington, Indiana 47405, United States*

**Xinfeng Gao** − *Department of Chemistry, Indiana University, Bloomington, Indiana 47405, United States*

**Maren Pink** − *Department of Chemistry, Indiana University, Bloomington, Indiana 47405, United States*

**Chun-Hsing Chen** − *Department of Chemistry, Indiana University, Bloomington, Indiana 47405, United States;* orcid.org/0000-0003-0150-9557

**Veronica Carta** − *Department of Chemistry, Indiana University, Bloomington, Indiana 47405, United States*

**Pierre Moënne-Loccoz** − *Department of Chemical Physiology and Biochemistry, School of Medicine, Oregon Health & Science University, Portland, Oregon 97239, United States;* orcid.org/0000-0002-7684-7617

Complete contact information is available at: https://pubs.acs.org/10.1021/acscentsci.0c00944


### Author Contributions

All authors have given approval to the final version of the manuscript.

### Notes

The authors declare no competing financial interest.

CCDC 2006945−2006959 contains the supplementary crystallographic data for this paper. These data can be obtained free of charge from The Cambridge Crystallographic Data Centre via www.ccdc.cam.ac.uk/structures.

## ACKNOWLEDGMENTS

J.L.M., S.A.L., and J.M.S acknowledged funding from the NSF (CHE-1566258 and CHE-1900020). P.M.-L. was supported by funding from the NIH (GM074785). Support for the acquisition of the Bruker Venture D8 diffractometer through the Major Scientific Research Equipment Fund from the President of Indiana University and the Office of the Vice President for Research is gratefully acknowledged. NSF's ChemMatCARS Sector 15 is supported by the Divisions of Chemistry (CHE) and Materials Research (DMR), National Science Foundation, under Grant NSF/CHE-1834750. Use of the Advanced Photon Source, an Office of Science User Facility operated for the U.S. Department of Energy (DOE) Office of Science by Argonne National Laboratory, was supported by the U.S. DOE under Contract DE-AC02-06CH11357.

## REFERENCES


(1) Turner, B. E.; Bally, J. Detection of Interstellar PN: The First Identified Phosphorus Compound in the Interstellar Medium. *Astrophys. J.* **1987**, *321*, L75−L79.

(2) Curry, J.; Herzberg, L.; Herzberg, G. Spektroskopischer Nachweis und Struktur des PN-Moleküls. *Eur. Phys. J. A* **1933**, *86*, 348−365.

(3) Curry, J.; Herzberg, L.; Herzberg, G. Spectroscopic Evidence for the Molecule PN. *J. Chem. Phys.* **1933**, *1* (10), 749−749.

(4) Atkins, R. M.; Timms, P. L. The Matrix Infrared Spectrum of PN and SiS. *Spectrochim. Acta* **1977**, *33A*, 853−857.

(5) Zhu, C.; Eckhardt, A. K.; Bergantini, A.; Singh, S. K.; Schreiner, P. R.; Kaiser, R. I. The Elusive Cyclotriphosphazene Molecule and its Dewar Benzene−Type Valence Isomer ($P_3N_3$). *Sci. Adv.* **2020**, *6*, eaba6934.

(6) Ahlrichs, R.; Bär, M.; Plitt, H. S.; Schnöckel, H. The Stability of PN and $(PN)_3$. Ab Initio Calculations and Matrix Infrared Investigations. *Chem. Phys. Lett.* **1989**, *161*, 179−184.

(7) Piro, N. A.; Figueroa, J. S.; McKellar, J. T.; Cummins, C. C. Triple-Bond Reactivity of Diphosphorus Molecules. *Science* **2006**, *313*, 1276−1279.

(8) Scherer, O. J. $P_x$ Units as Complex Ligands. *Comments Inorg. Chem.* **1987**, *6*, 1−22.

(9) Atkins, R. M.; Timms, P. L. Interaction of PN with Metal Atoms in a Krypton Matrix. *Inorg. Nucl. Chem. Lett.* **1978**, *14*, 113−115.

(10) Courtemanche, M. A.; Transue, W. J.; Cummins, C. C. Phosphinidene Reactivity of a Transient Vanadium PN Complex. *J. Am. Chem. Soc.* **2016**, *138* (50), 16220−16223.

(11) Smith, J. M.; Subedi, D. The structure and reactivity of iron nitride complexes. *Dalton Trans.* **2012**, *41* (5), 1423−9.

(12) Ding, M.; Rouzieres, M.; Losovyj, Y.; Pink, M.; Clerac, R.; Smith, J. M. Partial nitrogen atom transfer: a new synthetic tool to design single-molecule magnets. *Inorg. Chem.* **2015**, *54* (18), 9075−80.

(13) Martinez, J. L.; Lin, H. J.; Lee, W. T.; Pink, M.; Chen, C. H.; Gao, X.; Dickie, D. A.; Smith, J. M. Cyanide Ligand Assembly by Carbon Atom Transfer to an Iron Nitride. *J. Am. Chem. Soc.* **2017**, *139* (40), 14037−14040.

(14) Mösch-Zanetti, N. C.; Schrock, R. R.; Davis, W. M.; Wanninger, K.; Seidel, S. W.; O'Donoghue, M. B. Triamidoamine Complexes of Molybdenum and Tungsten That Contain Metal-E (E = N, P, and As) Single, Double, or Triple Bonds. *J. Am. Chem. Soc.* **1997**, *119*, 11037−11048.

(15) Zanetti, N. C.; Schrock, R. R.; Davis, W. M. Monomeric Molybdenum and Tungsten Complexes That Contain a Metal-Phosphorus Triple Bond. *Angew. Chem., Int. Ed. Engl.* **1995**, *34*, 2044−2046.

(16) Hoeft, J.; Tiemann, E.; Törring, T. Rotationsspektrum des PN. *Z. Naturforsch., A: Phys. Sci.* **1972**, *27a*, 703−704.

(17) Wyse, F. C.; Manson, E. L.; Gordy, W. Millimeter Wave Rotational Spectrum and Molecular Constants of 31P14N. *J. Chem. Phys.* **1972**, *57* (3), 1106−1108.

(18) Kinjo, R.; Donnadieu, B.; Bertrand, G. Isolation of a Carbene-Stabilized Phosphorus Mononitride and Its Radical Cation ($PN^{+\bullet}$). *Angew. Chem., Int. Ed.* **2010**, *49*, 5930−5933.

(19) Scepaniak, J. J.; Harris, T. D.; Vogel, C. S.; Sutter, J.; Meyer, K.; Smith, J. M. Spin Crossover in a Four-Coordinate Iron(II) Complex. *J. Am. Chem. Soc.* **2011**, *133* (11), 3824−7.

(20) O'Donoghue, M. B.; Davis, W. M.; Schrock, R. R. Derivatization of Dinitrogen by Molybdenum in Triamidoamine Complexes. *Inorg. Chem.* **1998**, *37*, 5149−5158.

(21) O'Donoghue, M. B.; Davis, W. M.; Schrock, R. R.; Reiff, W. M. Heterobimetallic Dinitrogen Complexes That Contain the $\{[N_3N]Mo\text{-}N{=}N\}^-$ Ligand. *Inorg. Chem.* **1999**, *38*, 243−252.

(22) Foster, J. P.; Weinhold, F. Natural Hybrid Orbitals. *J. Am. Chem. Soc.* **1980**, *102*, 7211−7218.

(23) Bader, R. F. W. A Quantum Theory of Molecular Structure and Its Applications. *Chem. Rev.* **1991**, *91*, 893−928.

(24) Johnson, M. J. A.; Odom, A. L.; Cummins, C. C. Phosphorus Monoxide as a Terminal Ligand. *Chem. Commun.* **1997**, 1523−1524.
(25) Westcott, S. A.; Stringer, G.; Anderson, S.; Taylor, N. J.; Marder, T. B. Synthesis, Structure, and Reactivity of RhCl(PhP-$\{CH_2CH_2PPh_2\}_2$). *Inorg. Chem.* **1994**, *33*, 4589−4594.



https://dx.doi.org/10.1021/acscentsci.0c00944
*ACS Cent. Sci.* 2020, 6, 1572−1577